32nd International Thermal Conductivity Conference
20th International Thermal Expansion Symposium
April 27–May 1, 2014
Purdue University, West Lafayette, Indiana, USA

Designing a Mechanically Robust Thermoelectric Module for High Temperature Application

Amirkoushyar Ziabari, aziabari@purdue.edu
Birck Nanotechnology Center, Purdue University; Electrical and Computer Engineering, Purdue University
Kazuaki Yazawa, kyazawa@purdue.edu
Birck Nanotechnology Center, Purdue University
Ali Shakouri, shakouri@purdue.edu
Birck Nanotechnology Center, Purdue University; Electrical and Computer Engineering, Purdue University

ABSTRACT

We report a numerical study on the impacts of variations in the geometry, boundary conditions, and the coefficient of thermal expansion of the materials on the maximum shearing stress in thermoelectric power generator module (TEM) for high temperature applications. The maximum shearing stress in the TEM is evaluated for different designs focusing on their dependency on the fill factor. Although predictions by the previously developed analytical modeling are in partial agreement with numerical results, simplifying assumptions for the analytical model can limit the range of validity. Our numerical analysis shows that reduction of the fill factor alone under all the circumstances will not reduce the maximum shear stress. Imposing mechanical constraints at the boundaries, increasing the number of legs (6×6 in the analysis), and engineering the coefficient of thermal expansion are some of the key parameters controlling the maximum shearing stress and its changes with the fill factor.

Keywords: thermoelectric module, shear stress, fill factor.

1. INTRODUCTION

For every unit of energy that is converted into electricity, more than one or two units of energy are not used in power plants today. This excess energy is primarily wasted as heat or thermal energy. Deploying systems to recover this wasted heat back into the energy stream is a wide spread topic of research. Thermoelectric generators (TEGs) are emerging as a possible solution for high temperature energy conversion applications and waste heat recovery systems. The key challenges are improving the efficiency of thermoelectric power generator module (TEM) and its material cost in large scale production. A system optimization for TE waste heat recovery system and minimization of the TEM cost is presented in Yazawa and Shakouri (2011). The closed form analytical solution reveals that the optimum solution for the maximum output power can be obtained by both electrical and thermal impedance matching and together with their heat source and the heat sink (hot and cold reservoirs). Upon finding the optimum solution, cost-performance analysis is conducted to find the minimum cost design at a given system efficiency. This optimization elucidates that the fractional area coverage of the TE leg, called fill factor or *FF*, plays a significant role in minimizing the mass of the TE material used in TE waste heat recovery systems. It is shown in Yazawa and Shakouri (2011) that improving the figure-of-merit (ZT) along with decreasing the FF would further reduce the total cost. Because the maximum power output from a TE system is proportional to square of temperature difference between the hot and cold reservoirs (Yazawa & Shakouri, 2012), employing a TE generator with optimum design in high temperature applications and with large temperature difference, such as on top of a steam turbine cycle, will be an economical approach to increase energy production (Yazawa, Koh, & Shakouri, 2013). However, both reduced FF and higher temperature range imply a larger impact on thermomechanical reliability. Elevated thermal stresses are viewed today as major bottlenecks for reliability and robustness in high temperature TEM applications. These stresses are caused by the significant differences in temperature between the “hot” and the “cold” substrate plates in a TEM design. The thermal stress problem can be solved by selecting adequate thermoelectric materials (Clin, Turenne, Vasilevskiy, & Masut, 2009; Gao, Du, Zhang, & Jiang, 2011) as well as by finding effective ways to reduce the stress level (Suhir & Shakouri, 2012). Using analytical and numerical modeling in Suhir and Shakouri, (2012) and Ziabari, Suhir, and Shakouri (2014), it is demonstrated that by reducing FF as well as using compliant interface materials, one can

DOI: 10.5703/1288284315556

reduce the maximum shearing stress occurring at the contacts. The maximum shear stresses are supposedly responsible for the structural robustness of the TEM assembly (Suhir & Shakouri, 2012). Reduction of the maximum shear stress by decreasing FF is not universal, and it depends on other parameters, such as the coefficients of thermal expansion (CTEs) of the different layers and the structural boundary conditions for the TEM assembly. In this work, we used finite element analysis to study how the geometry, structural boundary conditions, and the CTE of the materials in the TEM structure would change the maximum shear stress particularly in a high temperature application. In Section 2, we show the maximum shear stress obtained by analytical model developed in Suhir and Shakouri (2012, 2013) for a TEM designed for high temperature applications. In Section 3, we present the results obtained by finite element analysis software, ANSYS. We will also discuss how different parameters affect the maximum shear stress in the TEM structure. Finally, we will conclude in Section 4.

2. THERMAL STRESS IN TE MODULES

A schematic of a TE module proposed for high temperature application is shown in Figure 1 (Suhir & Shakouri, 2013). The substrate components and metallization layers are made of molybdenum (Mo) alloys. The rest of material properties and dimensions are listed in Table 1. The pitch distance between legs is set to 200 μm. By changing the width of the TE legs, the FF can be changed. Similar to Suhir and Shakouri (2013), analytical equations (Equation 1) for a simplified six leg model, shown in Figure 1(b), are developed to calculate maximum shear stress in the structure.

$$\tau_{max} = k\frac{\alpha\Delta t}{\lambda_1}\tanh kl\left[1+\frac{\left(\tanh kl+\coth kl+8kl\left(\frac{L}{2l}-1\right)\right)}{\left(\left(\tanh kl+\coth kl+4kl\left(\frac{L}{2l}-1\right)\right)^2+8kl\left(\frac{L}{2l}-1\right)\tanh kl+\left(4kl\left(\frac{L}{2l}-1\right)^2\right)\right)\sinh 2kl}\right] \quad (1)$$

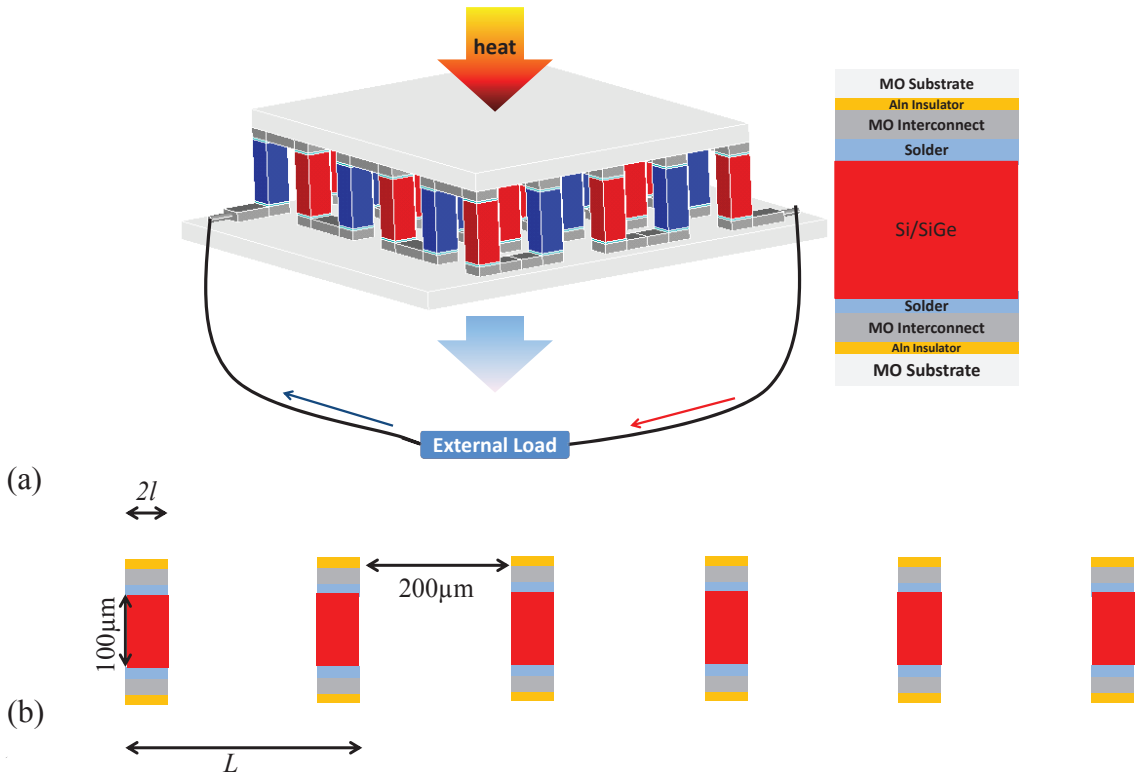

Figure 1. (a – left) Schematic of a thermoelectric generator, (a – right) and materials proposed for different layers for high temperature applications (Suhir & Shakouri, 2013); (b) Simplified 2D model used for analytical modeling.

Table 1. Material properties and dimension for the proposed TEM for high temperature

Material	Thickness (μm)	Young Modulus (Gpa)	CTE (10^{-6}/°C)	Poisson Ratio	Yield Stress (GPa)	Ultimate Stress (GPa)
Mo alloy	50	330	4.8	0.31	–	–
AIN insulator	0.05	330	6.58	0.24	–	–
Mo interconnect	30	330	4.8	0.31	–	–
Solder	5	78.5	14.2	0.42	200	220
Si/SiGe TE	100	250	2.6	0.28	–	–

$$k = \sqrt{\frac{2\lambda_1}{\kappa}} \tag{2}$$

$$\lambda_1 = \frac{1 - v_1}{E_1 h_1} \tag{3}$$

In these equations, k is the parameter of the interfacial shearing stress, κ is the total interfacial shear compliance of the midlayers between the two top and bottom components, α (1/°C), v_1, E_1 (GPa), and $h_1(m)$ are the coefficient of thermal expansion (CTE), Poisson ratio, modulus of elasticity, and the thickness of the substrate component, respectively, Δt is temperature difference between the hot and the cold sides, λ_1 is the axial compliance of one of the bonded components, L is end-to-end distance between the two legs, and l is the half width of TE leg. Major assumptions in obtaining the equations are listed in Suhir and Shakouri (2012) and Ziabari et al. (2014).

The maximum shear stress takes place at the end of the peripheral legs. Maximum shear stress as a function of FF is graphed in Figure 2, assuming temperature at the hot and the cold sides are 800°C and 630°C ($\Delta t = 170$). A 2× reduction the in maximum shear stress is obtained by decreasing FF from 25% to about 3%. The maximum shear stress is plotted for two different values of CTE for substrate layer, so that we can compare the results with the corresponding numerical results in the next section.

Although analytical modeling gives an intuition on the parameters contributing to the maximum shear stress, it has some key assumptions (Suhir & Shakouri, 2012), which impose limitations on the accuracy of the calculated thermal stresses. It assumes a homogenous CTE in all the layers and does not consider any local CTE mismatch between the layers. The analysis is two dimensional (2D) but takes into account the three dimensional (3D) state of stress in an approximate fashion by bringing in the Poisson ratio and elastic modulus of the substrate layer (Ziabari et al., 2014). Additionally, it assumes that the assembly is thick and stiff enough, so that

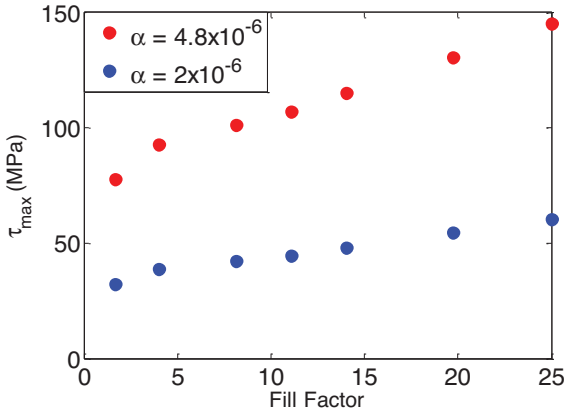

Figure 2. Analytical modeling result for maximum shear stress as a function of fill factor in variations of α (CTE of Mo Substrate).

it does not experience bending deformations, or, if it does, bending does not affect the interfacial thermal shearing stresses and does not need to be accounted for. In the next section, we exploited ANSYS to carry out 3D finite element analysis and identify how each of these unaccounted parameters would contribute to the maximum interfacial shear stress in the assembly.

3. NUMERICAL RESULTS AND DISCUSSIONS

Three-dimensional (3D) structural-thermal analysis is carried out in ANSYS to calculate thermal stresses in TEMs. Twenty node Solid226 tetrahedral elements are used for meshing of the structure. The material properties are according to the Table 1. Homogenous CTE equal to 2×10^{-6} is assumed among the layers, unless otherwise stated. We performed all the simulations with three different FF of 25%, 11% and 4%, corresponding to leg widths of 100 μm, 50 μm, 25 μm, respectively. The pitch distance between the legs is set to be 200 μm. Also, temperature at the hot and the cold sides is assumed 800°C and 630°C ($\Delta t = 170$).

A two leg simple 3D model for the TE module is constructed and numerical analysis is conducted. The maximum shear stress takes place at the interface

with the Mo substrate. This maximum shear stress, at the top and bottom Mo/AlN interfaces, is plotted against FF for three different boundary conditions in Figure 3(a) and (b). Free-standing structure and constraint on the perpendicular translation at either the hot, or the cold side are the three boundary conditions considered. 1.5× to 2.5× reduction in the maximum shear stress by decreasing the FF by 8× is obtained for different boundary conditions, which confirms the results of analytical modeling shown in Figure 2. Stress values for the 3D model are lower than those of obtained with 2D analytical model which is also reasonable. The maximum shear at the Mo/AlN interface is due to the rigidity and the large modulus of the insulator material. In practice, this large stress can be avoided by utilizing a thin compliant interface between the two layers. Therefore, the main concern is the maximum shear stress at the interconnect/solder interface. In Figure 3(c) and (d), the maximum shear stress at the top and bottom interconnect/solder interfaces, for the same structure under the same boundary conditions, are plotted against FF. It is evident from these figures that the maximum shear stress is reduced as FF decreases. In all the cases, the maximum shear under the free-standing boundary condition is lower than the other cases. When we impose constraint on perpendicular translation at the hot surface, the maximum shear at the top interface (closer to the hot side) is larger while it stays almost the same on the cold side. Limiting the expansion of the hot side generates stronger stresses on this side. However, the stress can be relaxed along the legs towards the cold side, resulting in similar stress values compared with the unconstrained case. On the contrary, when we impose constraint on the cold interface, the maximum shear stress took place at the bottom interface (closer to the cold side), and the stress on the top interface remains similar to the free-standing case.

It is apparent from Figures 3(a)–(d) that the two cases of imposing constraint at the hot and the cold sides are complementary to each other, and studying one of them would be sufficient to understand the other. Therefore, in the rest of analysis, we only show the result for the free-standing case as well as the case with perpendicular constraint on *y*-translation at the cold side. Also, since interconnect/solder interface is more prone to thermo-mechanical failure, due to solder's low yield stress, we will show the results for maximum shear at this interface.

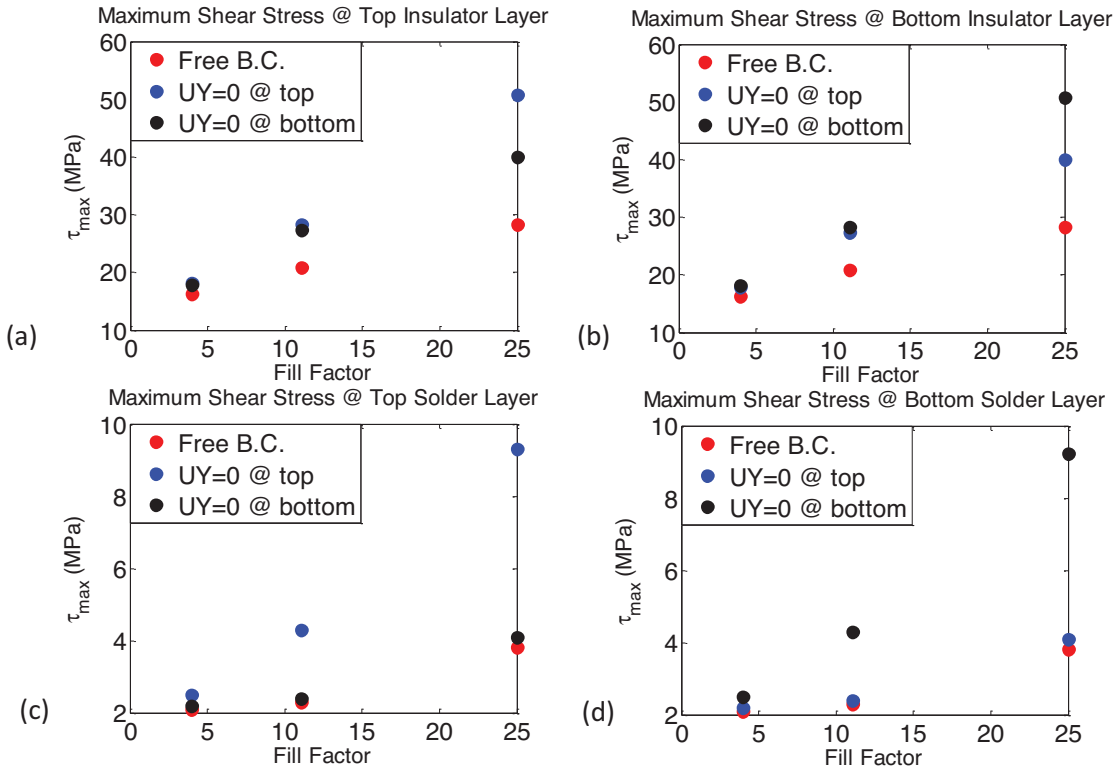

Figure 3. Maximum shear stress against fill factor for three different boundary conditions of free standing (blue), perpendicular translation is constrained at the top hot side (red), perpendicular translation is constrained at the bottom cold side (green). Maximum shear stresses are probed (a) at the top component/insulator interface; (b) at the bottom component/insulator interface; (c) at the top interconnect/solder interface; (d) at the bottom interconnect/solder interface.

In order to understand thermal stress behavior in a more realistic configurations, we performed three dimensional finite element analysis on 6 legs as well as an array of 6 × 6 legs (36-legs) structures (Figure 1(a)). Again, we are interested in the maximum shear stress at the interface of the interconnect and the solder layer. Figure 4 reveals how the trends of maximum shear against FF vary for different cases of 2-legs, 6-legs, and 36-legs structures and different boundary conditions. For the case with free-standing boundary condition, the maximum shear for a two legs simplified model would drop by reducing the FF, while the trends for the cases of 6 legs and 36-legs reverse and the maximum shear rises by decreasing the FF. For large FFs, the maximum shear stress for the three structures is not different. However, at small FFs the maximum shear stress is significantly different between 2-leg and multileg structures. This is mainly due to the asymmetric bending of the two large substrates. The outward/inward expansion of the hot and the cold substrates will deform the TE leg of the low FF structure and generate strong shear stresses.

If we anchor the bottom surface to limit the perpendicular translation at the cold side, the expansion of the bottom substrate would be limited and trends would be the same for different structures. This is shown in Figure 4(b).

Shear stress distribution for 36-legs structure under both boundary conditions and for the 2-leg TEM in free-standing case is demonstrated in Figure 5. This figure elucidates why the trends are different for 36-legs and 2-legs in a free standing structure. Figure 5(a)–(f) show that by varying the FF from 11% to 4% in a 2-leg design the leg bending decreases (5a, 5b), while this increases for 36-leg design (5e, 5f). As a result, the maximum shear stress has an opposite trend in the two cases. Also, Figures 6(c) and 5(d), illustrate that

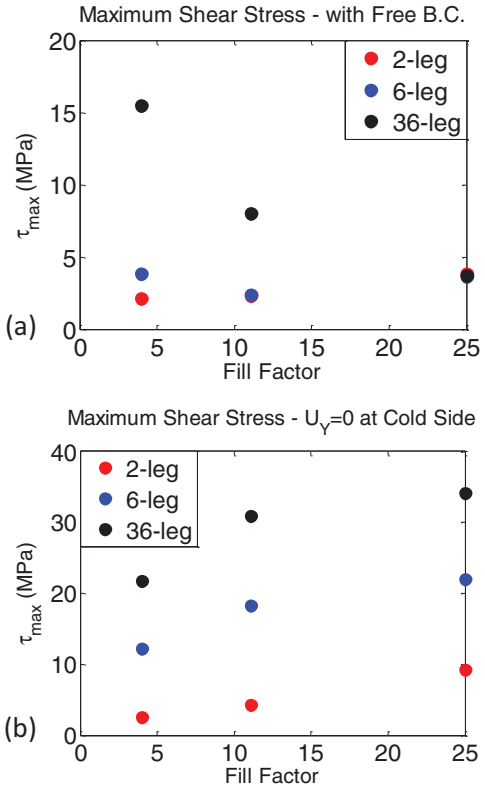

Figure 4. Maximum shear stress at the interconnect/solder interface against Fill Factor for three different structures with (a) free-standing boundary condition; (b) perpendicular translation is constrained at the bottom interface.

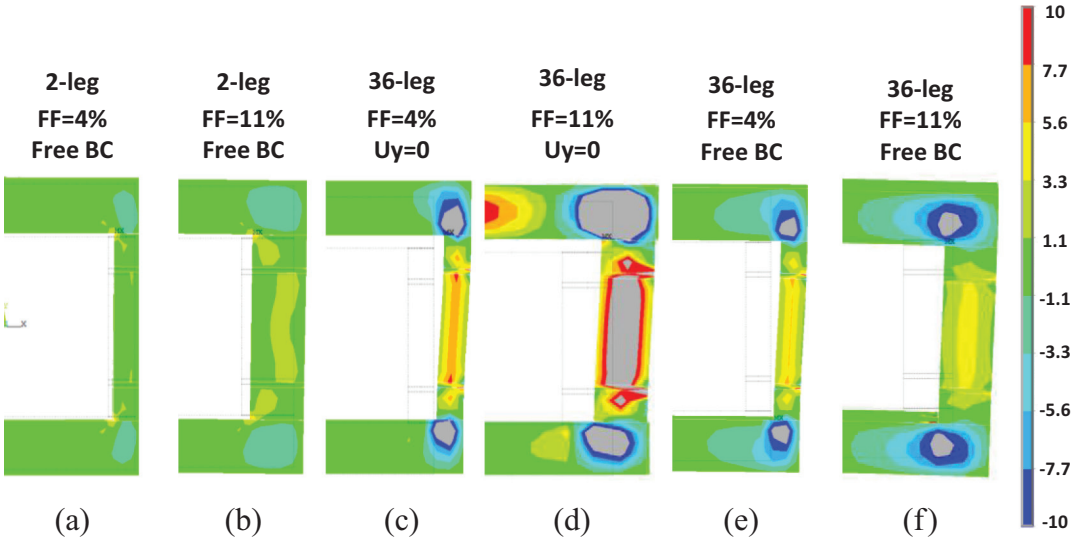

Figure 5. Shear stress distribution in TEM structures. Maximum and minimum are capped at ±10 MPa. (a) Free-standing two-leg TEM with FF = 4%; (b) free-standing two-leg TEM with FF = 11%; (c) 36-leg TEM constrained at the cold side with FF = 4%; (d) 36-leg TEM constrained at the cold side with FF = 11%; (e) free-standing 36-leg TEM with FF = 4%; (c) free-standing 36-leg TEM with FF=11%.

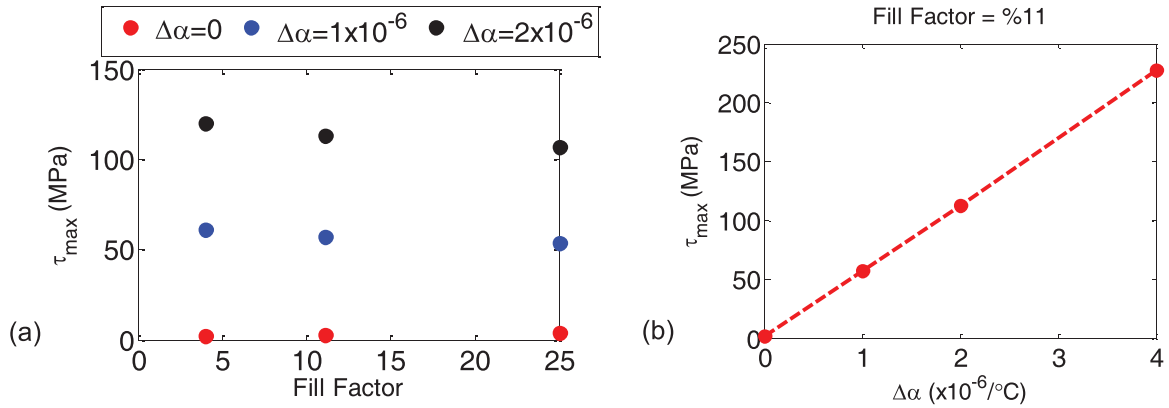

Figure 6. (a) Trend of maximum shear stress against FF for different CTE mismatches between the solder and its neighboring layers; (b) Maximum shear in TEM vs. CTE mismatch between solder and TE leg material.

when the perpendicular translation is restrained at the cold side, strong stresses is generated on that side. These stresses are larger for the case with larger FF and relax in the leg toward the hot side. Therefore, larger FF with constrained boundary condition in 36-leg design has larger stress compared to lower FF, which also oppose the trend for the case shown in Figures 5(e) and 6(f), but follows the analytical predictions.

In the previous analysis, a homogenous CTE among the materials used in the TEM structure is assumed. While this assumption is not realistic, it gives us an intuition on what is the sole outcome of varying geometrical factors under certain boundary conditions. Under homogenous CTE, only temperature difference between the top and the bottom substrates provoke the maximum shear stress in the structure. However, localized CTE mismatch between the layers could adversely affect the maximum shear stress in the structure and can result in large failure even at small FFs. Figure 6(a) shows how the trend of maximum shear stress against FF for different CTE mismatches between the solder and its neighboring layers. When there is no mismatch, the trend is decreasing and the stress values are low. However, a slight mismatch at high temperature could generate strong stresses as well as changes the trend how stress scales with the FF. Figure 6(b) shows that the maximum shear stress varies linearly with the difference between CTE of the solder and the TE leg material ($\Delta\alpha$), if CTE in all the other layers remains constant.

4. CONCLUSIONS

A large temperature difference between the hot and cold substrates in TEMs could result in large local thermomechanical stresses and possible mechanical failure. Analytical model presented in this work and the previous works give some initial trends how geometry can affect the maximum shear stress. Based on these modeling, decreasing FF by a factor of 8 in a TEM from 25% to 3%, could result in more than 2× reduction in the maximum shear stress. This is in agreement with the results obtained by 3D finite element analysis of a 2-leg TEM structure assuming homogenous CTE in all of the layers. Imposing structural boundary condition on either the hot or cold side of the structure does not change the predicted trend. However, this constraint leads to generation of a stronger shear stress in the contact near the constrained side compared to the free-standing case. The stress will relax toward the unconstrained side. In designing TE module for high temperature applications, it is not always sufficient to look at the simplest design. Depending on the boundary conditions, modules with multiple legs might produce different results compared to the simple two leg design. CTE mismatch between the layers could produce significant local shear stress at the high temperature situation. This local stress should be proportional to $\Delta\alpha\Delta T$. This effect could be mitigated by changing the geometry or choosing material properties that are closely matched.

REFERENCES

Clin, T., Turenne, S., Vasilevskiy, D., & Masut, R. A. (2009). Numerical simulation of the thermomechanical behavior of extruded bismuth telluride alloy module. *Journal of Electronic Materials, 38*, 994–1001. doi:10.1007/s11664-009-0756-9.

Gao, J.-L., Du, Q.-G., Zhang, X.-D., & Jiang, X.-Q. (2011). Thermal stress analysis and structure parameter selection for a Bi2Te3-based

thermoelectric module. *Journal of Electronic Materials*, *40*(5), 884–888. doi:10.1007/s11664-011-1611-3.

Suhir, E., & Shakouri, A. (2012). Assembly bonded at the ends: could thinner and longer legs result in a lower thermal stress in a thermoelectric module design?. *Journal of Applied Mechanics*, *79*(6), 061010.

Suhir, E., & Shakouri, A. (2013). Predicted thermal stress in a multileg thermoelectric module (TEM) design. *Journal of Applied Mechanics*, *80*, 021012. doi:10.1115/1.4007524.

Yazawa, K., Koh, Y. R., & Shakouri, A. (2013). Optimization of thermoelectric topping combined steam turbine cycles for energy economy. *Applied Energy*, *109*, 1–9. doi:10.1016/j.apenergy.2013.03.050.

Yazawa, K., & Shakouri, A. (2011). Cost-efficiency trade-off and the design of thermoelectric power generators. *Environmental Science & Technology*, *45*, 7548–7553. doi:10.1021/es2005418.

Yazawa, K., & Shakouri, A. (2012). Optimization of power and efficiency of thermoelectric devices with asymmetric thermal contacts. *Journal of Applied Physics*, *111*, 024509. doi:10.1063/1.3679544.

Ziabari, A., Suhir, E., & Shakouri, A. (2014). Minimizing thermally induced interfacial shearing stress in a thermoelectric module with low fractional area coverage. *Microelectronics Journal*, *45*, 547–553. doi:10.1016/j.mejo.2013.12.004.